

Molecular opacities for low-mass metal-poor AGB stars undergoing the Third Dredge Up

S. Cristallo and O. Straniero

INAF-Osservatorio Astronomico di Collurania, 64100 Teramo, Italy

M. T. Lederer and B. Aringer

Institut für Astronomie, Türkenschanzstraße 17, A-1180 Wien, Austria

ABSTRACT

The concomitant overabundances of C, N and s-process elements are commonly ascribed to the complex interplay of nucleosynthesis, mixing and mass loss taking place in Asymptotic Giant Branch stars. At low metallicity, the enhancement of C and/or N may be up to 1000 times larger than the original iron content and significantly affects the stellar structure and its evolution. For this reason, the interpretation of the already available and still growing amount of data concerning C-rich metal-poor stars belonging to our Galaxy as well as to dwarf spheroidal galaxies would require reliable AGB stellar models for low and very low metallicities. In this paper we address the question of calculation and use of appropriate opacity coefficients, which take into account the C enhancement caused by the third dredge up. A possible N enhancement, caused by the cool bottom process or by the engulfment of protons into the convective zone generated by a thermal pulse and the subsequent huge third dredge up, is also considered. Basing on up-to-date stellar models, we illustrate the changes induced by the use of these opacity on the physical and chemical properties expected for these stars.

Subject headings: stars: AGB and post-AGB — stars: atmospheres — stars: carbon — stars: evolution

1. Introduction

The modification of the surface composition of a star may be due to several processes. If the synthesis of nuclei occurs in stellar interiors, the products of nuclear reactions only appear at the surface when this chemically enriched material is moved from the deepest

layers to the external zone. The most common deep-mixing processes are caused by convective instabilities. Less studied, but not less important, are dynamical instabilities induced by rotation or by magnetic forces (see e.g. Maeder & Meynet 2000). Minor surface chemical alterations occur on a longer timescale, as those due to microscopic diffusion, levitation powered by radiation pressure or other thermal instabilities (Kippenhahn & Weigert 1990, see also Piersanti et al. 2007, and references therein). The first systematic modification of the surface composition takes place at the base of the red giant branch, when the external convection penetrates the zone previously exposed to the H burning. This is the so called *first dredge up* (FDU). Later on, during the early Asymptotic Giant Branch, intermediate mass stars ($4 < M/M_{\odot} < 8$) eventually experience a *second dredge up*. The main effect on the surface composition of these two dredge-up episodes is the increase of the He abundance. A redistribution of the CNO isotopes also occurs, namely isotopes with a slow proton capture (e.g. ^{14}N) become more abundant, whereas those whose proton capture is fast are depleted (e.g. ^{12}C). In any case, after the first and the second dredge up the global number of CNO isotopes is conserved. This is not the case of the *Third Dredge Up* (TDU). Actually, TDU refers to multiple dredge up episodes occurring during the late part of the AGB. In these stars, recursive Thermal Pulses (TPs) are powered by violent He ignitions, which take place at the base of the thin He-rich zone located between the CO core and the H-rich envelope (intershell). These violent He burning episodes cause the intershell to become unstable against convection and therefore to mix the products of the 3α burning throughout this region. Shortly after each thermal pulse, the H-burning dies down (owing to the expansion initiated to counterbalance the excess of energy released by the 3α reactions) and the external convection may penetrate down to the H-exhausted region. Thus, the stellar envelope is enriched with the ashes of the He burning, mainly ^{12}C . This carbon dredge up is of great importance for the future AGB evolution. Indeed, the efficiency of the CNO cycle and that of the radiative energy transfer are both depending on the carbon abundance in the envelope. During the AGB, owing to the carbon enhancement, the opacity increases and, in turn, the temperature gradient becomes larger¹. In practice, since as a consequence of the C dredge up the C/O becomes rapidly greater than 1, the effective temperature decreases, the stellar radius increases and the average mass loss rate increases, thus eroding at a faster rate the envelope mass. On the other hand, the growth in mass of the H-exhausted core, which is controlled by the H burning, also depends on the amount of C (and N) in the envelope. As shown by Straniero et al. (2003), changes of the core and the envelope masses affect all the fundamental properties of AGB stars, such as the thermal pulse strength or the total amount of mass that is dredged up.

¹In the external convective zone of an AGB stars, the radiative flux significantly contributes to the overall energy transport.

In the more massive AGB stars ($M > 4 M_{\odot}$), an additional phenomenon should be considered. In these stars, indeed, the temperature at the base of the convective envelope may become large enough ($T > 5 \times 10^7$ K) for the activation of the CN cycle. In this case, the C excess in the envelope is partially converted into N. This process is known as *Hot Bottom Burning* (Sugimoto 1971; Iben 1973).

In principle, a stellar evolution code should account for the variations of the envelope chemical composition. In practice, only variations of the main constituents are usually considered. In particular, low temperature radiative opacity tables are available only for scaled solar composition, so that only changes of H and He can be accounted for. Although the use of these tables substantially underestimates the radiative opacity of the cool atmosphere of an evolved AGB star eventually enriched in C and N, they are commonly adopted by stellar modelers, who are often left without any other alternative.

Marigo (2002) made a first step towards a correct description of the abundance changes in the calculation of opacity coefficients, by estimating molecular concentrations through dissociation equilibrium calculations. Although the results of this work definitely demonstrate the importance of a correct opacity treatment, its simplified approach suffers from some drawbacks, in particular the limited number of molecular species included.

In this paper, we make a further step ahead. By interpolating on a grid of opacity tables properly computed by increasing the abundances of C and N with respect to the scaled solar value, we calculate new models for low mass AGB stars. We start with a very metal poor composition ($[\text{Fe}/\text{H}] < -2$), because the effect of the TDU is stronger in this case. Observational constraints for these models come from the so-called CEMP (Carbon Enhanced Metal Poor) stars, for which C/Fe ratios even larger than 10^3 have been observed. Actually, they are not AGB stars, but unevolved dwarfs belonging to wide binary systems, which have been polluted by the wind of an AGB companion (see e.g. Lucatello et al. 2005). The majority of these CEMP stars also show huge nitrogen enhancements. A slow deep circulation, perhaps driven by rotation-induced instabilities or by the formation of magnetic pipes connecting the base of the convective envelope to the region where the CN cycle takes place, is generally considered responsible for the partial conversion of C into N in low mass AGB stars. After Wasserburg et al. (1995) this phenomenon has been called *Cool Bottom Process* (CBP). However, nitrogen enhancements can also be produced in very metal poor stars by a peculiar thermal pulse occurring at the beginning of the TP-AGB phase, when the abundances of CNO isotopes in the envelope are particularly low. As firstly proposed by Hollowell et al. (1990) (see also Iwamoto et al. 2004 and Straniero et al. 2004), in such a case the convective zone generated by this anomalous thermal pulse may extend up to the base of the H-rich envelope. Protons, captured by convection, are rapidly mixed within

the intershell, where the high temperature and the large C abundance induce a violent H-burning flash. For a short time, up to 10^{42} erg/sec are released by the CN cycle. Thus, in the intershell zone, a substantial amount of ^{14}N (and ^{13}C) is produced. Later on, after a particularly deep TDU, the envelope is enriched with both C and N. If $\text{C/O} > 1$, a large N abundance, in addition to the C enhancement, favors the formation of CN molecules, thus inducing a further increase of the radiative opacities in the cool atmospheres of AGB stars. In Section 2 we discuss in more detail the new opacity tables. New models for low mass AGB stars undergoing the TDU are presented in Section 3, while in Section 4 we compare models with only carbon dredge up and models where both C and N are enhanced. A final discussion follows.

2. Molecular opacities

In the cool layers (i. e. temperatures lower than about 4000 K) of the convective envelope and of the atmosphere of late-type stars, molecules become the dominant opacity source. Beside the local thermodynamic conditions, the concentration of the various molecular species basically depends on the atomic abundances. In this respect, an important quantity is the carbon to oxygen number ratio. Among the various molecular species involving C atoms, CO have indeed the larger dissociation energy, so that for $\text{C/O} < 1$ almost all the C atoms participate to the formation of this molecule, while the oxygen atoms in excess are free to form other molecules. For M stars, the C/O ratio is below unity, i. e. they are "oxygen-rich". During the TP-AGB phase these stars can be turned, depending on their mass and metallicity, into S-type ($\text{C/O} \simeq 1$) and subsequently into carbon-rich objects (N stars with $\text{C/O} > 1$), as a consequence of the TDU. In this case, the carbon atoms in excess forms new molecules. The atmospheric structure of an O-rich stars does significantly differ from that of a C-rich star, as different molecules contribute to the opacity: TiO and H_2O are most important in the oxygen-rich regime, while carbon-bearing molecules (e. g. C_2 , CN, C_2H_2 and C_3) dominate the opacity for $\text{C/O} > 1$.

Current model atmosphere codes (e. g. hydrostatic MARCS models (Gustafsson et al. 1975) or dynamic models (Höfner et al. 2003)) generally include molecular opacity data that are suitable for M-type stars as well as for C-type stars. On the contrary, most stellar evolution models of AGB stars ignore the opacity changes caused by the TDU. Recently, the OPAL collaboration² as well as the Opacity Project³ provided web tools to calculate Rosseland mean

²<http://www-phys.llnl.gov/Research/OPAL/opal.html> .

³<http://opacities.osc.edu/> .

opacities. Unfortunately, they are limited to the atomic contributions and do not include the most important molecular photon absorbers (except H_2). Below 10^4 K, the Rosseland mean tables presented by Alexander & Ferguson (1994), which are available for scaled solar compositions only, are widely used.

In order to improve our AGB models and to evaluate the effects of the chemical modifications caused by the TDU and, eventually, by the CBP, we have calculated a grid of opacity tables by means of the COMA code from Aringer (2000), based on molecular data given in Tab. 1. Atomic opacities have been derived from VALD (Kupka et al. 2000). We have generated a set of tables for different mass fractions of hydrogen, helium, carbon and nitrogen. The abundances of all the other elements have been scaled with respect to the corresponding solar values, namely $X_* = X_\odot \times Z_*/Z_\odot$, where $Z_* = 1 \times 10^{-4}$ and X_* refer to the stellar model composition. As reference solar composition we adopt Anders & Grevesse (1989), with some exceptions (C and N from Allende Prieto et al. 2002, while O, Ne and Ar from Asplund et al. 2004). In order to cover the large overabundances observed in CEMP stars, we calculate tables where C and N have been independently multiplied up to a factor of 2000 (with intermediate enhancements of 10, 100 and 500), taking into account all the possible combinations. Temperatures has been varied to cover the parameter space of the cool external layers of an AGB star ($3.2 < \log T < 4.05$). We have used the OPAL web tool to extend the opacity tables at temperature larger than $\log T = 4.05$. Cubic interpolations in $\log T$ and $\log R^4$ and linear interpolations in the mass fractions of H, C and N ensure a sufficient accuracy in the evaluation of the opacity coefficients. We decide to first compute C- and N-enhanced opacity tables at $Z = 1 \times 10^{-4}$ because the effects induced by the carbon dredged up in the envelope is maximized at low metallicity. However, we plan to prepare C- and N-enhanced tables covering a larger metallicity range and to collect them in a database.

The differences between opacities calculated for scaled solar composition and opacities calculated by enhancing C and N are illustrated in Figs. 1 and 2. As shown in Fig. 1, an enhancement of carbon and nitrogen due to the third dredge up leads to a C- (and N-) rich mixture whose opacities are more than two orders of magnitude larger than the initial ones over a wide range of temperature and density. In this Figure, we also compare our initial scaled solar opacity to the corresponding values from Alexander & Ferguson (1994). The overall agreement is quite good. The significant discrepancy at low temperature/high density is due to the inclusion of dust absorption in Alexander & Ferguson (1994). Even though the stellar models here considered never attain the physical conditions for dust grain formation in their atmospheres, we want to point out that, for the astrophysical scenario

$^4R = \rho \times 10^{18} / T^3$.

under consideration, dust formation is far from equilibrium; usually much less dust than under equilibrium conditions is formed (Gail & Sedlmayr 1988). In Fig. 2 we point out the differences between the mean opacity coefficients for a scaled solar composition (case A, derived from Alexander & Ferguson 1994) and a corresponding table where only the C and N abundances are enhanced (case B). Particularly, in case B we start from a scaled solar mixture with a metallicity of $Z=10^{-4}$ and then we enhance the mass fraction of ^{12}C by a factor of 500 and the mass fraction of ^{14}N by a factor of 10, thus attaining a total metallicity $Z=8.5\times 10^{-3}$ (the same as in case A). In the oxygen-rich case A, H_2O and TiO dominate the opacity at low temperatures. For high densities, the Rosseland mean is higher than in the carbon-rich case B, whereas the opposite is true for lower densities. In this region carbon-bearing molecules are the dominant opacity source (see below and cf. Fig. 3). In the region from $\log T \simeq 3.3$ to $\log T \simeq 3.8$ (depending on $\log R$), atomic opacities significantly contribute to the Rosseland mean. Consequently, case A comprises higher opacities in this region as more metals (apart from C and N) are present than in case B.

The most important contributions in the Rosseland mean opacities of a C-rich mixture are due to CN, C_2 , C_2H_2 , and C_3 . These molecules contribute to the mean opacity in different regions of the parameter space ($\log T, \log R$) (see Fig. 3). In particular, C_2H_2 dominates the low temperature high density region, while C_3 provides the main photon absorption at low T and low R , but only for extreme C-rich mixture. At higher temperatures ($3000 < T < 4000$) and densities the opacity is mainly controlled by CN and C_2 , and the relative contribution between these two molecules also depends on the amount of nitrogen. Note that, at variance with solar metallicity, in metal poor stars, even considering the nitrogen enhancement resulting after the first dredge up, the CN molecules may contribute to the opacity only if primary nitrogen is added, as in the case of many CEMP stars.

Finally, we have also investigated the influence of a moderate increase of the oxygen mass fraction. Compared to the effects of the carbon enhancement, this contribution was found to be negligible. For this reason, variations of the O abundance were not included into our set of tables.

3. C-enhanced models

As outlined in the previous section, molecules are the dominant opacity source in the range $3.3 < \log T < 3.6$. These temperatures are usually attained in the most external layers of AGB stars. As far as we know, the extant AGB stellar models are based on low temperature opacity tables calculated for scaled solar compositions and only the variation of the relative abundance of H and He is generally taken into account. Perhaps, some investigators

could have approximated the effect of dredged-up by using opacities appropriate to the new total Z value. However, while this approximation may be adequate to follow the evolution of AGB progenitors, the occurrence of recursive TDU episodes and the consequent enhancement of C in the envelope requires particular attention. The inadequacy of scaled solar opacity coefficients for AGB stellar models is particularly severe in metal poor calculations, where the overall mass of C that is dredged up may be 1000 times larger than the whole initial metal content (Z), whereas the iron content practically remains equal to the initial one.

In our previous calculations (Cristallo 2006, Straniero et al. 2006), attempting to mimic the effect of the C enhancement on the opacity, we choose to linearly interpolate on Z , the overall mass fraction of elements with atomic number ≥ 6 . In that case, we didn't allow for possible relative variations among these elements. Actually, the material that is dredged up by convection is mainly composed by freshly synthesized C, while other heavy elements, as iron, remain practically unchanged. Thus, such a global metallicity interpolation overestimates the atomic iron contribution to the opacity, whereas underestimates the carbon (atomic and molecular) contribution. Since these different atomic and molecular opacity sources operates in distinct stellar layers, it is rather difficult to evaluate, a priori, how much the contributions from these two different sources of opacity may compensate each other.

In this Section we compare stellar models with initial mass $M=2M_{\odot}$, initial helium $Y=0.245$ and initial metallicity $Z=1\times 10^{-4}$ (or $[\text{Fe}/\text{H}]=-2.17$), as obtained under different assumptions about opacity. To calculate the corresponding evolutionary sequences, we have used the FRANEC stellar evolution code (the release described in Chieffi et al. 1998). Mixing and mass loss algorithms for the AGB phase are those described in Straniero et al. (2006). In particular, we derive the mass loss rate for AGB models basing on the observed correlation with the pulsational period (Schöier & Olofsson 2001, Whitelock et al. 2003). Periods are estimated from the P - M_K relation proposed by Feast et al. (1989)⁵.

We discuss, in particular, three different models, namely:

1. the *Z-fixed* model, where only variations of He/H are considered (the metallicity is always maintained equal to the initial value);
2. the *Z-int* model, where variations of He/H and Z are considered, but the elemental distribution of heavy elements is always maintained scaled solar;

⁵Bolometric corrections from Fluks et al. (1994) have been used.

3. the *CN-int* model, which properly takes into account variations of He/H, C and, eventually, N caused by the TDU. All the other elements are maintained to their initial (scaled solar) values.

Let us remark that the three models have been computed with identical input physics, except the opacity coefficients, and that the three evolutionary sequences have been followed up to the last TDU episode.

Fig. 4 clearly shows the huge difference in AGB evolution resulting from different opacity calculations. The first direct consequence of the introduction of a growing envelope opacity in the *Z-int* and *CN-int* models is the evident drop of the effective temperature. The temperature gradient is indeed linearly dependent on the opacity coefficient. For a given luminosity, this occurrence implies a larger radius as well as a larger mass loss rate. As a result, the duration of the TP-AGB phase is significantly shortened. This effect is however overestimated in the *Z-int* model with respect to the more appropriate *CN-int* model.

A second important consequence of the different treatment of the low temperature opacity concerns the chemical yields. The amount of mass that is dredged up after a thermal pulse (δM_{TDU}) basically depends on the core mass and on the envelope mass and both of them are affected by a variation of the envelope opacity. The evolution of the three calculated δM_{TDU} are illustrated in Fig. 5. They initially increase, because the core mass increases, reach a maximum and, then, decrease, because the mass loss erodes the envelope mass. However, since the growth of the mass loss is steeper in the *Z-int* and *CN-int* models, the total mass that is dredged up is lower than that found in the case of the *Z-fixed* model. As a result, models computed with larger opacity predict a smaller contribution to the galactic chemical evolution.

Cristallo (2006) already noted that the overabundances of the heavy elements synthesized by the s process in the *Z-int* model are generally too small compared to the available spectroscopic determination for C- and s-rich metal poor stars belonging to the galactic halo. Such a discrepancy appears more severe, considered that these halo stars are not AGB stars undergoing the TDU, but less evolved objects, dwarfs or red giants, whose envelopes have been polluted by the wind of already evolved AGB companions. After the rapid accretion process, the C- and s- enriched material has been diluted by convection, in case of giant stars, or by secular processes, as microscopic diffusion or thermohaline mixing, in case of dwarf stars (see e.g. Stancliffe et al. 2007). We concluded that the opacity is overestimated in these models, causing a too large mass loss and a too short TP-AGB phase.

A longer TP-AGB phase, with more dredge up episodes and, in turn, with larger final overabundances of the s-elements, are obtained in the case of the *Z-fixed* model, but in

this case the effective temperature, always greater than 4200 K (see the upper curve in Fig. 4), would not match the observed temperatures of metal poor C(N) stars found in dwarf spheroidal galaxies, typically ranging between 3500 and 4000 K (Domínguez et al. 2004).

An inspection of Fig. 5 shows that the *CN-int* model, which undergoes 15 TDU episodes, represents an intermediate case between the *Z-int* model (9 TDU) and the *Z-fixed* model (48 TDU). The total amount of mass that is dredged up is $3.8 \times 10^{-2} M_{\odot}$, $9.7 \times 10^{-2} M_{\odot}$ and $1.9 \times 10^{-1} M_{\odot}$ in the *Z-int*, *CN-int* and *Z-fixed* model, respectively. Even if the *CN-int* model shows lower overabundances with respect the *Z-fixed* model, the drop of its effective temperature caused by the C dredge up matches the low values found for metal poor C(N) stars in dwarf spheroidal galaxies. It appears, therefore, that the inconsistency between surface temperatures and s-process enhancement could be solved by using appropriate opacity coefficients. A detailed comparison between the prediction of our AGB models and the observed elemental overabundances in CEMP stars will be presented in a forthcoming paper.

4. C- and N-enhanced models

In massive AGB ($M > 4 M_{\odot}$) the temperature at the base of the convective envelope is large enough to convert part of the C dredged up into N (the so called Hot Bottom Burning). This is not the case of low mass AGB, although some authors postulated the existence of a slow circulation, named Cool Bottom Process (CBP), capable to mix the material within the thin layer located between the H-burning shell and the cool base of the convective envelope (see Nollett et al. 2003, and references therein). While it is widely accepted that the CBP operates during the RGB, mainly because low mass red giant stars show low values of the $^{12}\text{C}/^{13}\text{C}$ ratio (Gratton et al. 2000), its activation during the AGB still remains a matter of debate. Up to date, the origin of CBP has not been clearly identified, but the magnetic field could play a relevant role for the activation of this process (Busso et al. 2006). If the CBP would be at work in low mass AGB, it might be responsible for the conversion of C into N. Actually, many CEMP stars show large N enhancements. However, as already recalled, a huge N enhancement might be also produced if the convective zone generated by a thermal pulse ingests protons from the top, a possibility early recognized by Hollowell et al. (1990), who claimed that this process should be rather common in very metal poor stars. We are preparing a paper where we describe the evolution and the nucleosynthesis of these models. Preliminary results indicate that it exists a maximum mass for which such a peculiar thermal pulse takes place and that this limit increases as the metallicity decreases. In Fig. 6, the asterisk represents the initial input parameters of the models presented here.

Our interest, in the context of this paper, is related to the possible consequences induced

by the N enhancement on the properties of low-mass low-metallicity AGB stars. A first indication about the difference between a C-rich and a CN-rich envelope can be deduced from Fig. 7. Here, starting from the physical structure of the *CN-int* model after the 4th and the 14th pulse with TDU, we calculate, without a re-adjustment of the stellar structure, the opacity coefficients assuming that one half of the ¹²C has been converted into ¹⁴N. The resulting percentage differences with respect to the original opacity of the *CN-int* model (those calculated taking into account the C dredge up only) have been reported.

The important differences found at low temperature are due to the absorbtion of the CN molecules, whose contribution to the opacity is marginal in the *CN-int* model. This effect is larger toward the end of the AGB phase, because the surface temperature drops down to 3500 K (logT=3.55), where the CN contribution is maximum (see Fig. 3).

In order to better characterize the influence of the N enhancement, four additional AGB models have been computed, by introducing an extra-circulation below the base of the convective envelope. As shown by Domínguez et al. (2004), the most important parameter of the CBP is the maximum temperature at which the circulated material is exposed (T_{max}), while the actual rate of circulation is significantly less important. Then, in the four models here presented, the circulation rate is taken constant and fixed to 1/1000 of the average turbulent velocity of the most internal layers within the convective envelope (corresponding to $v_{conv} \sim (20 \div 100) \text{ cm} \cdot \text{s}^{-1}$), while the mass extension of the extra-circulation is varied so that $T_{max}=30, 40, 50$ and 60×10^6 K in model *CN-int-30*, *CN-int-40*, *CN-int-50* and *CN-int-60*, respectively. The extra-circulation has been switched on at the beginning of the TP-AGB phase and it remains active only if the energy flux released by the H-burning is larger than that of the He-burning (*i.e.* during the interpulse phase).

When $T_{max} \geq 40 \times 10^6$ K, the larger opacity caused by the ¹⁴N production from CBP makes the surface temperature lower with respect to the standard (*i.e.* *CN-int*) model (for $T_{max} = 30 \times 10^6$ K no appreciable differences have been found). This implies a more efficient mass loss and a shorter TP-AGB phase. The *CN-int-40* model experience 12 TDU episodes, 11 the *CN-int-50* model and 9 the *CN-int-60* model. The total masses that are dredged up are $7.6 \times 10^{-2} M_{\odot}$, $6.6 \times 10^{-2} M_{\odot}$ and $6.3 \times 10^{-2} M_{\odot}$, respectively.

The envelope chemical composition is significantly affected by the introduction of the CBP, the surface nitrogen abundance being greatly enhanced with respect to the standard case. In Fig. 8, we report the evolution of the [C/N] ratio versus the [C/Fe] ratio, in the usual spectroscopic notation, for the four models with CBP and the one without CBP.

All these models start the pre-main sequence with scaled solar abundance ratios, namely [C/Fe]=0 and [C/N]=0, whose values drop down to -0.31 and -0.74, respectively, after the

first dredge up. Then, the resulting saw-blade pattern of the various curves is due to the alternate action of the TDU and the CBP during the AGB phase. Indeed, $[C/Fe]$ and $[C/N]$ both increase after a TDU episode, whereas they decrease during interpulse periods, as a consequence of the CBP. The deeper the CBP is, the lower the final $[C/N]$ ratio is, spanning a range of about two order of magnitude (from $[C/N] \sim 2.2$ down to $[C/N] \sim -0.5$). Note that the $[C/N]$ of the CEMP stars, for which this ratio has been derived, typically ranges between 0 and 1 (Johnson et al. 2007).

5. Conclusions

In this paper we have discussed the use of appropriate opacity to describe the effects of the C enhancement caused by the third dredge up in low-mass-low-metallicity AGB stars. New opacity tables for chemical mixtures with different overabundances of C and N have been obtained by means of the COMA code (Aringer 2000). Then, stellar models with $M=2M_{\odot}$, $Y=0.245$ and $Z=1 \times 10^{-4}$ have been computed, varying the interpolation scheme on these tables. We have also discussed the consequence of the conversion of C into N, as eventually caused by the Cool Bottom Process operating in low mass AGB stars or by proton ingestion in the first Thermal Pulse of very low metallicity AGB stars.

Both the C dredge up and the conversion of C into N induce substantially affect the molecular contribution to the opacity for temperature lower than 4000 K. Larger opacity coefficients imply cooler envelopes, larger mass loss rate and, in turn, shorter AGB lifetime. It also affects the variation of the surface composition and the global yields produced by low mass AGB stars. The amount of mass that is dredged up is, indeed, influenced by the different temporal variation of the envelope mass.

We show that only models computed by adopting opacity that properly include the enhancements of C and, eventually, N can reproduce the photometric and spectroscopic properties of their observational counterparts. In particular, the low effective temperature (3500 \sim 4000 K) of the low metallicity C stars belonging to dwarf spheroidal galaxies can be naturally reproduced when the new opacity are used. These models can also account for the relatively large overabundance of heavy elements, those produced by the s-process nucleosynthesis, observed in C- and s-rich halo stars.

SC and OS have been supported by the Italian National Grant Program PRIN 2004. MTL has been supported by the Austrian Academy of Sciences (DOC-programme) and acknowledges funding through FWF project P18171.

REFERENCES

- Aaronson, M., & Mould, J.: 1985, ApJ, 290, 191.
- Alexander, D.R., & Ferguson, J.W.: 1994, ApJ, 437, 879.
- Allende Prieto, C., Lambert, D.L., Asplund, M.: 2002, ApJ, 573, 137.
- Alvarez, R., & Plez, B.: 1998, A&A, 330, 1109.
- Anders, E., & Grevesse, N.: 1989, Geochim. Cosmochim. Acta, 53, 197.
- Aringer, B.: 2000, *Ph.D. thesis*, University of Vienna.
- Asplund, M., Grevesse, N., Sauval, A.J., Allende Prieto, C., Kiselman, D.: 2004, A&A, 417, 751.
- Barber, R.J., Harris, G.J., Tennyson, J.: 2002, J. Chem. Phys., 117, 11239.
- Barber, R.J., Tennyson, J., Harris, G.J., and Tolchenov, R.N.: 2006, MNRAS, 368, 1087.
- Busso, M., Calandra, A., Nucci, M.C.: 2006, Mem. Soc. Astron. Italiana, 77, 798.
- Chieffi, A., Limongi, M., Straniero, O.: 1998, ApJ, 502, 737.
- Cristallo, S.: 2006, PASP, 118, 1360.
- Domínguez, I., Abia, C., Straniero, O., Cristallo, S., Pavlenko, Ya.V.: 2004, A&A, 422, 1045.
- Feast, M.W., Glass, I.S., Whitelock, P.A., Catchpole, R.M.: 1989, MNRAS, 241, 375.
- Fluks, M.A., Plez, B., The, P.S., de Winter, D., Westerlund, B.E.,
- Gail, H.-P., & Sedlmayr, E.: 1988, A&A, 206, 153.
- Goorvitch, D., & Chackerian, Jr.C.: 1994, ApJS, 91, 483.
- Gratton, R., Sneden, C., Carretta, E., Bragaglia, A.: 2000, A&A, 354, 169.
- Gustafsson, B., Bell, R.A., Eriksson, K., Nordlund, A.: 1975, A&A, 42, 407.
- Harris, G.J., Tennyson, J., Kaminsky, B.M., Pavlenko, Y.V., Jones, H.R.A.: 2006, MNRAS, 367, 400.
- Höfner, S., Gaultschy-Loidl, R., Aringer, B., Jørgensen, U.G.: 2003, A&A, 399, 589.
- Hollowell, D., Iben, I.Jr., Fujimoto, M.Y.: 1990, AJ, 351, 245.

- Iben, I.: 1973, ApJ, 185, 209.
- Irwin, A.W.: 1988, A&AS, 74, 145.
- Iwamoto, N., Kajino, T., Mathews, G.J., Fujimoto, M.Y., Aoki, W.: 2004, ApJ, 602, 377.
- Johnson, J.A., Herwig, F., Beers, T.C., Christlieb, N.: astro-ph/0608666
- Jørgensen, U.G., Almløf, J., Siegbahn, P.E.M.: 1989, ApJ, 343, 554.
- Jørgensen, U.G.: 1997, *Molecules in Astrophysics: Probes and Processes* IAU Symp. 178, Ed. van Dishoeck, E.F., p. 441.
- Kippenhahn, R. & Weigert, A.: 1990, *Stellar Structure and evolution*, Springer-Verlag, Berlin Heidelberg.
- Kupka, F.G., Ryabchikova, T.A., Piskunov, N.E., Stempels, H.C., Weiss, W.W.: 2000, BaltA, 9, 590.
- Langhoff, S.R., & Bauschlicher, C.W.: 1993, Chem. Phys. Lett., 211, 305.
- Lucatello, S., Tsangarides, S., Beers, T.C., Carretta, E., Gratton, R.G., Ryan, S.G.: 2005, ApJ, 625, 825.
- Maeder, A., & Meynet, G.: 2000, ARA&A, 38, 143.
- Marigo, P.: 2002, A&A, 387, 507.
- Nollett, K.M., Busso, M., Wasserburg, G.J.: 2003, ApJ, 582, 1036.
- Piersanti, L., Straniero, O., Cristallo, S.: 2007, A&A, 462, 1051.
- Querci, F., Querci, M., Tsuji, T.: 1974, A&A, 31, 265.
- Rossi, S.C.F., Maciel, W.J., Benevides-Soares, P.: 1985, A&A, 148, 93.
- Rothman, L.S. and 19 coauthors: 1998, *Journal of Quantitative Spectroscopy and Radiative Transfer*, 60, 665.
- Sauval, A.J., & Tatum, J.B.: 1984, ApJS, 56, 193.
- Schöier, F.L., & Olofsson, H.: 2001, A&AS, 368, 969.
- Schwenke, D.W.: 1997, private communication.

- Schwenke, D.W.: 1998, in *Chemistry and Physics of Molecules and Grains in Space. Faraday Discussions No. 109*, pp 321.
- Stancliffe, R.J., Glebbeek, E., Izzard, R.G., Pols, O.R.: 2007, *A&A*, 464, 57.
- Straniero, O., Domínguez, I., Cristallo, S., Gallino, R.: 2003, *PASA*, 20, 389.
- Straniero, O., Cristallo, S., Gallino, R., Domínguez, I.: 2004, *Mem. Soc. Astron. Italiana*, 75, 665.
- Straniero, O., Gallino, R., Cristallo, S.: 2006, *Nucl. Phys. A*, 777, 311.
- Suda, T., Aikawa, M., Machida, M.N., Fujimoto, M.Y., Iben, I.Jr.: 2004, *ApJ*, 611, 476.
- Sugimoto, D.: 1971, *Prog. Theor. Phys.*, 45, 761.
- Vidler, M., & Tennyson, J.: 2000, *J. Chem. Phys.*, 113, 9766.
- Wasserburg, G.J., Boothroyd, A.I., Sackmann, I.-J.: 1995, *ApJ*, 447, 37.
- Whitelock, P.A., Feast, M.W., van Loon, J.Th., Zijlstra, A.A.: 2003, *MNRAS*, 342, 86.

Table 1. Molecular Line Data

Molecule	Source of Thermodynamic Data	Number of Lines	Source of Line Data
CO	1	131,859	6
CH	2	229,134	7
C ₂	1	360,887	8
SiO	2	93,372	9
CN	1	2,533,040	7
TiO	1	22,758,691	10
H ₂ O	3	27,988,952	11
HCN/HNC	4	34,433,190	12
OH	1	38,068	13
VO	1	3,171,552	14
CO ₂	2	60,802	15
SO ₂	5	38,853	15
HF	1	107	15
HCl	1	533	15
C ₂ H ₂	-	opacity sampling	16
C ₃	-	opacity sampling	16

Note. — Molecules entering the calculation of the Rosseland mean opacity. References for thermodynamic and line data as indexed in columns two and four are given below. Atomic line data are taken from VALD (Kupka et al. 2000).

References. — (1) (Sauval & Tatum 1984); (2) (Rossi et al. 1985); (3) (Vidler & Tennyson 2000); (4) (Barber et al. 2002); (5) (Irwin 1988); (6) (Goorvitch & Chackerian 1994); (7) (Jørgensen 1997); (8) (Querci et al. 1974); (9) (Langhoff & Bauschlicher 1993); (10) (Schwenke 1998); (11) (Barber et al. 2006); (12) (Harris et al. 2006); (13) (Schwenke 1997); (14) (Alvarez & Plez 1998); (15) (Rothman et al. 1998); (16) (Jørgensen et al. 1989).

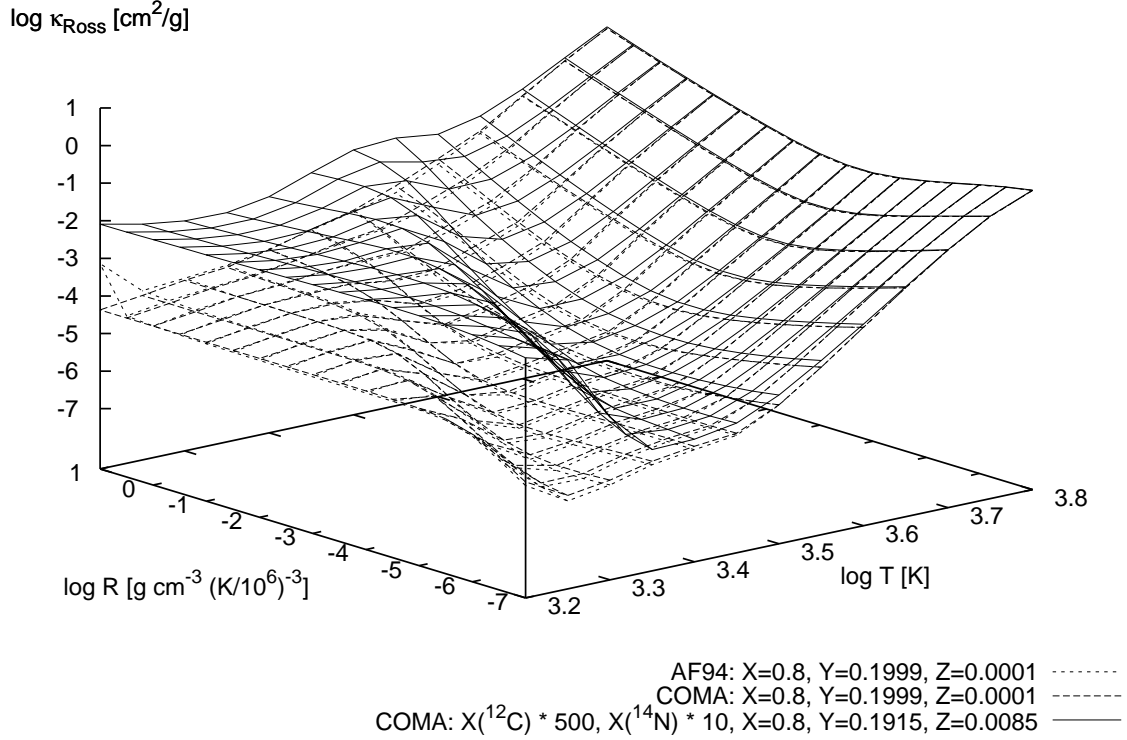


Fig. 1.— Rosseland mean opacity as a function of $\log T$ and $\log R$ in a range representative for the envelopes of AGB stars: dashed lines represent values for a chemical composition $X=0.8$, $Y=0.1999$, and $Z=0.0001$. As a comparison, the results of Alexander & Ferguson (1994), which are based on a different line data set, are shown (dotted lines); the strong discrepancy at low $\log T$ and high $\log R$ is due to grain opacity which is not included in our calculations. Enhancing the ^{12}C (and ^{14}N) mass fraction results in a significant increase of opacity (solid lines) in the cooler layers due to the favored formation of carbon-bearing molecules, especially CN and C_2H_2 .

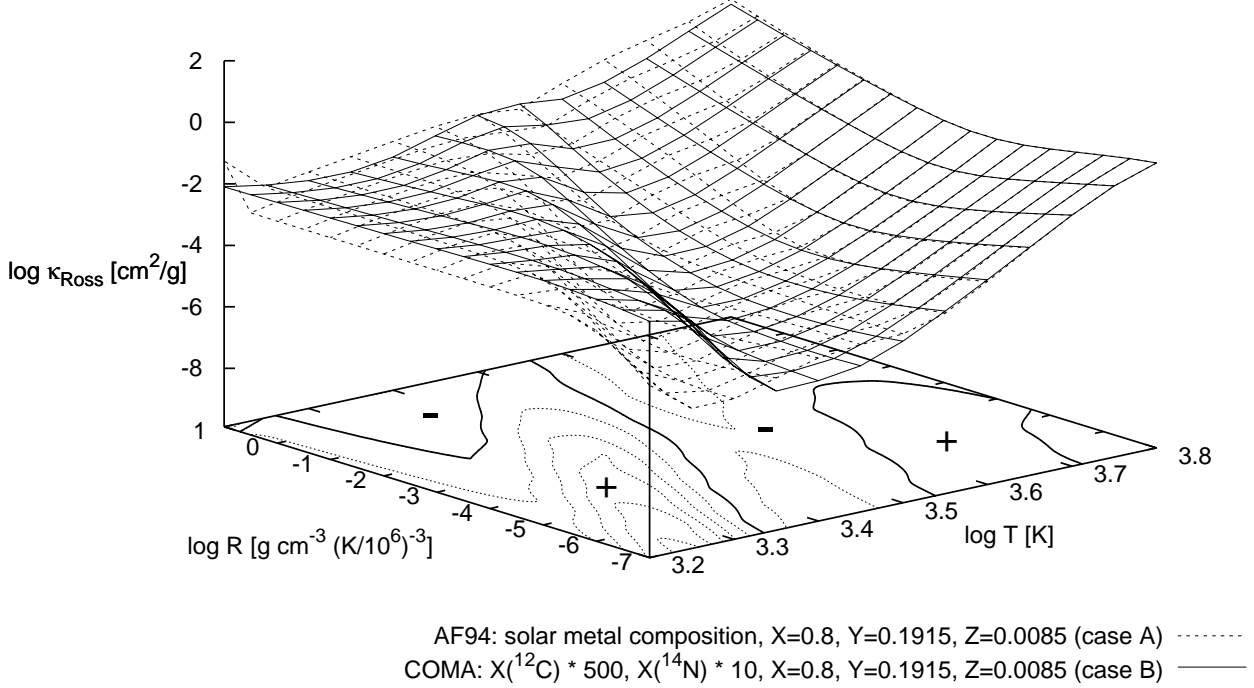


Fig. 2.— Comparison of the Rosseland mean opacity for two chemical mixtures with the same overall metallicity $Z=0.0085$. Case A is a mixture with solar scaled metal abundances (dashed lines). For case B only the mass fractions of ^{12}C and ^{14}N have been enhanced starting from a solar scaled mixture with $Z=0.0001$ (solid lines). The differences between the two tables are indicated by contour lines at the base of the plot. The thick line, at which in terms of opacity $B = A$, separates regions where $B > A$ and $B < A$, marked with + and – signs, respectively (dotted lines are separated from each other by steps of 0.5 dex). For case A, H_2O and TiO dominate κ_{Ross} at lower temperatures. At high densities, this leads to a higher mean opacity than in case B, whereas at low densities carbon-bearing molecules (cf. Fig. 3) cause an increase of the mean opacity of up to 2.5 dex compared to case A. Atomic opacities, relevant from $\log T \simeq 3.3$ to $\log T \simeq 3.8$ (depending on $\log R$), are higher in case A.

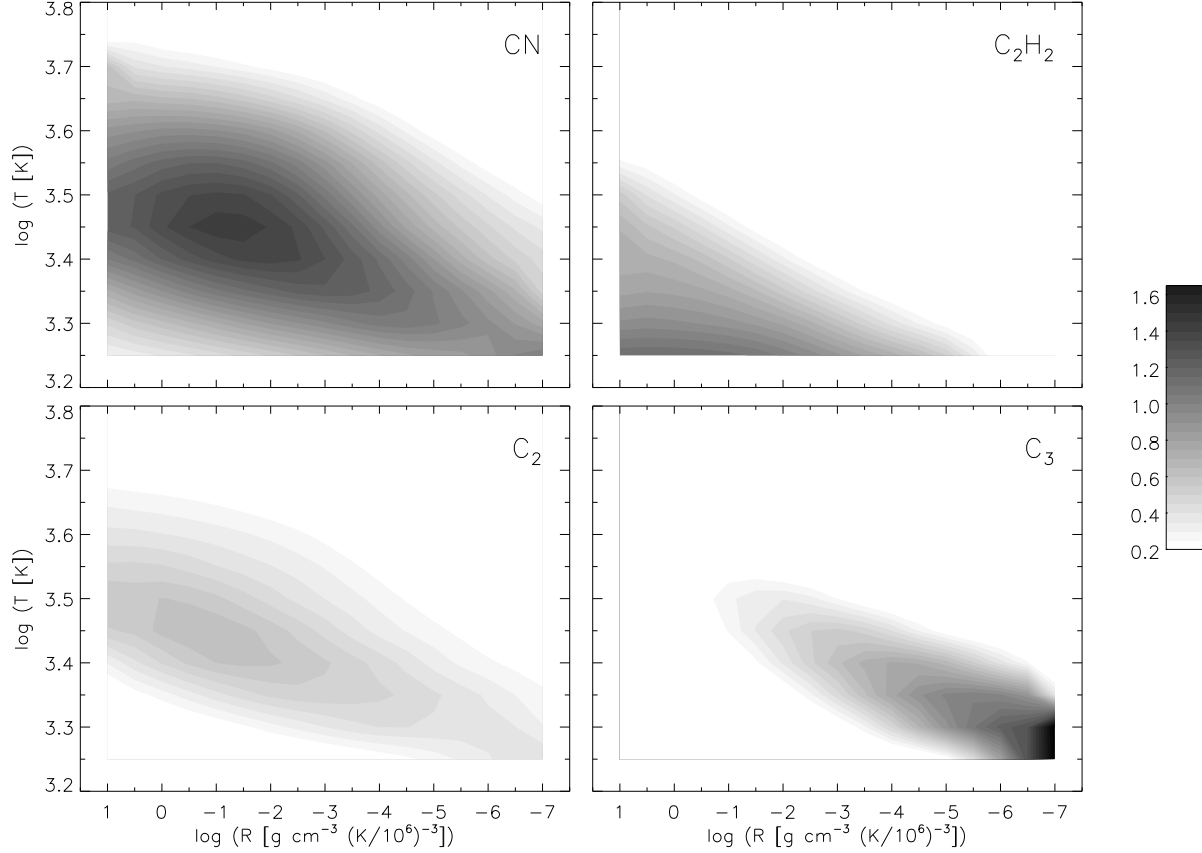


Fig. 3.— Contribution of molecular species to the Rosseland mean opacity: the plots show differences (in orders of magnitudes) between the total opacity and calculations where particular molecules (indicated in each panel) have been omitted. The extreme case of our grid (i.e. mass fraction of ^{12}C and ^{14}N enhanced by a factor of 2000) has been chosen as the basis for these figures, as in this way the regions where certain molecules contribute can be identified most clearly.

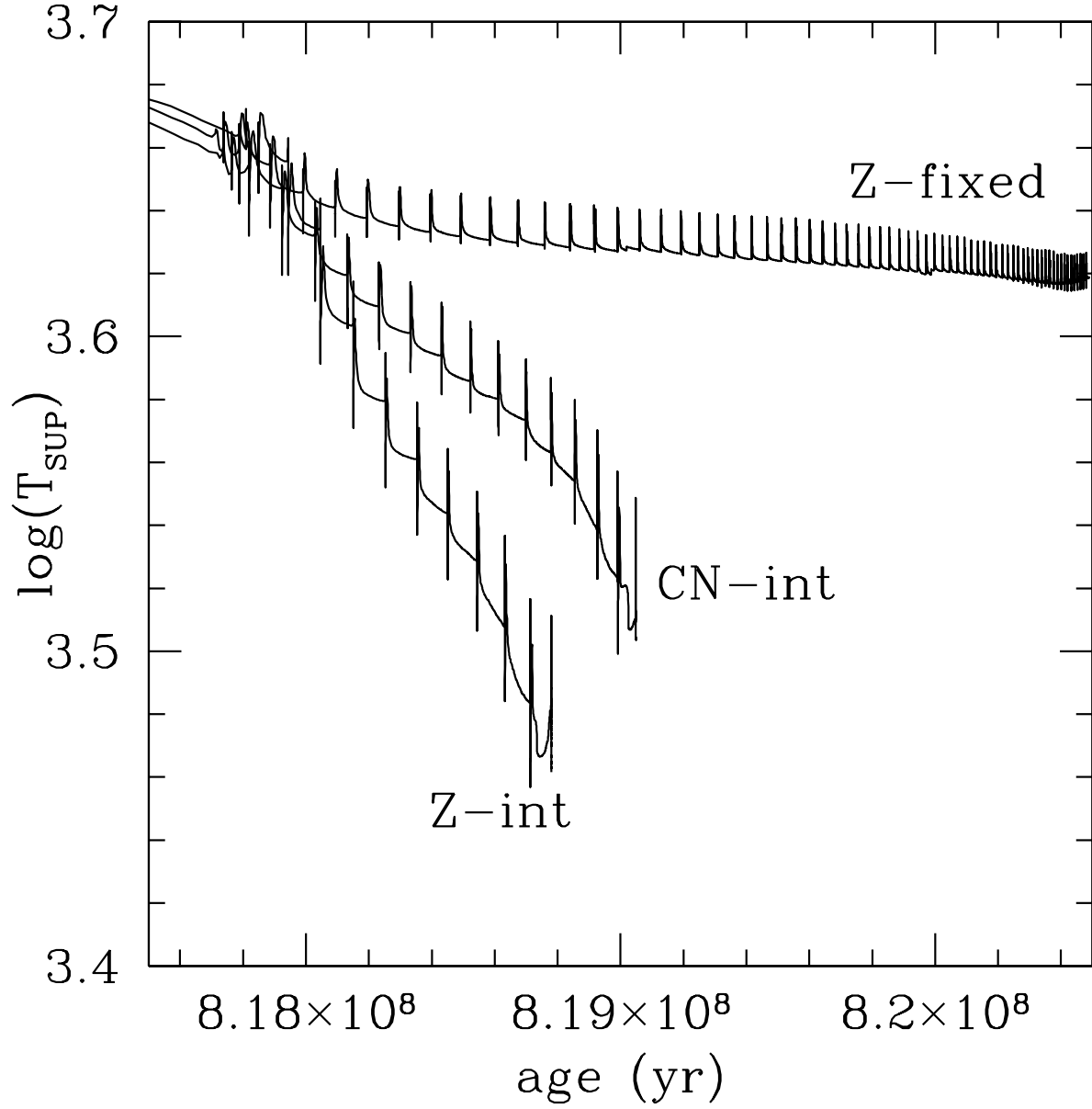


Fig. 4.— We report, for the three models discussed in the text, the surface temperature vs. age.

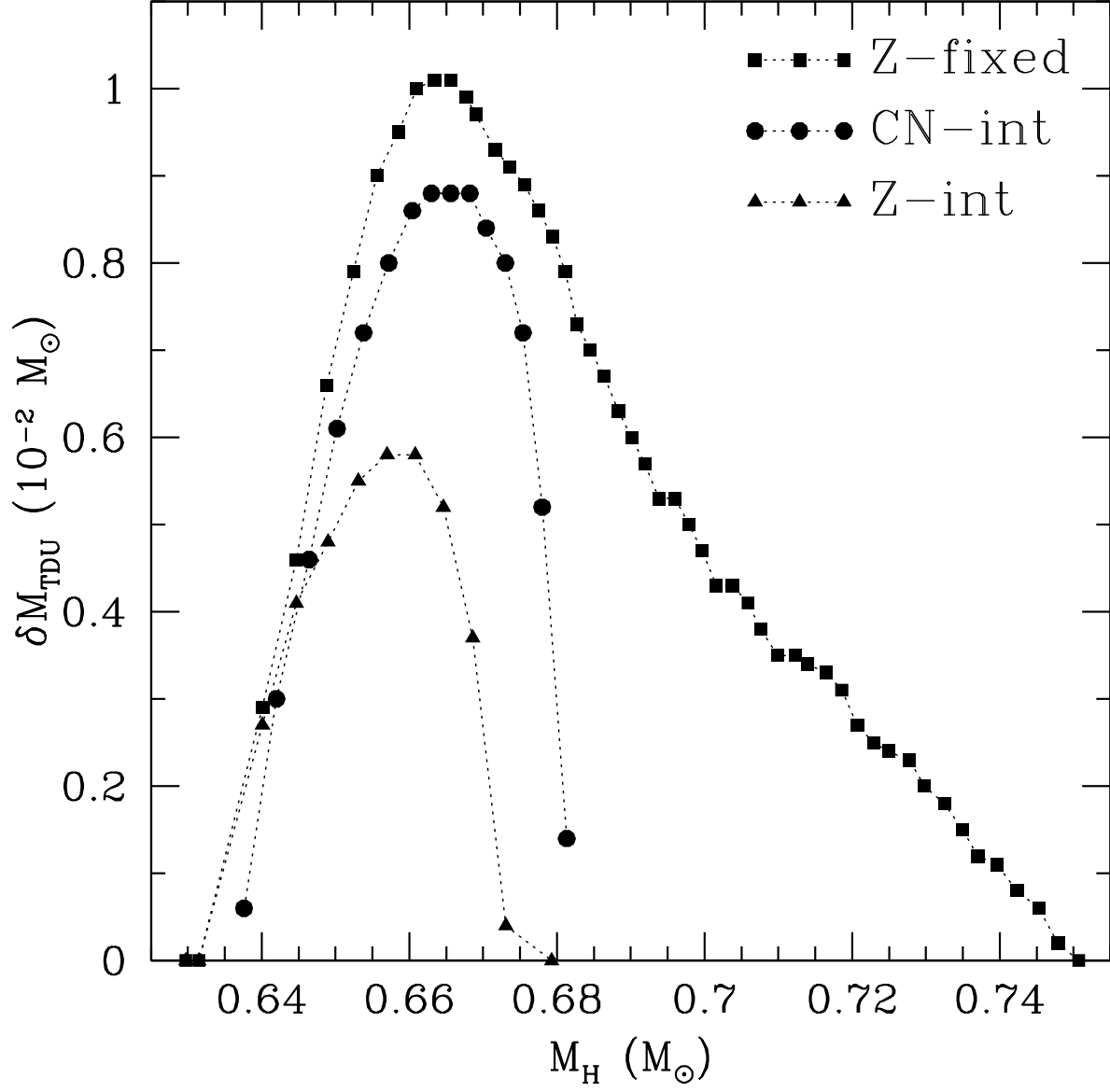


Fig. 5.— We report, for the three models discussed in the text, the dredged up material vs. core mass.

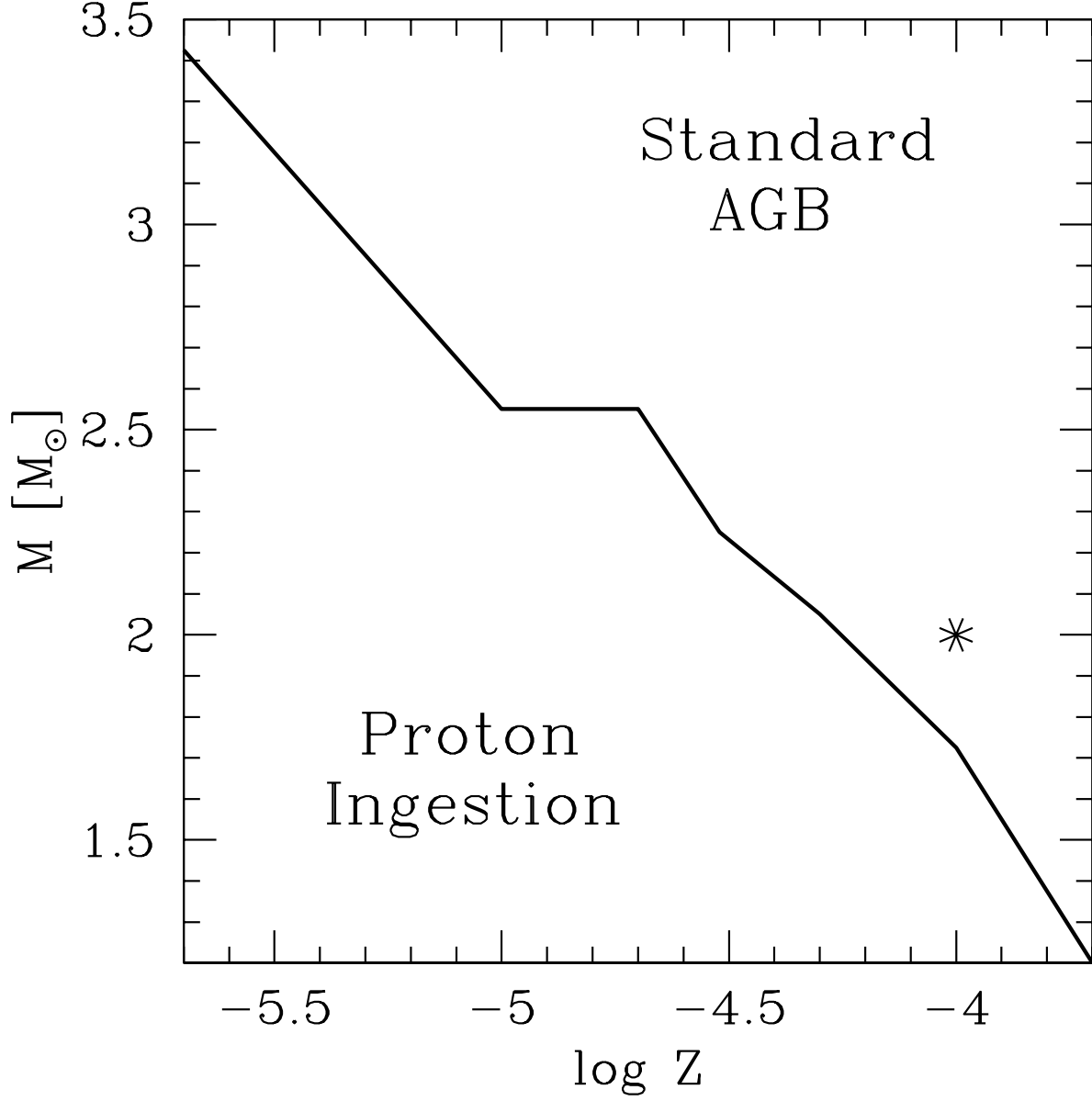


Fig. 6.— In a metallicity-mass diagram, we report the line that separates models following a standard AGB evolution (upper region) from that ones suffering a proton ingestion episode at the beginning of their AGB phase (lower region). The asterisk corresponds to the initial input parameters of the models presented in this paper.

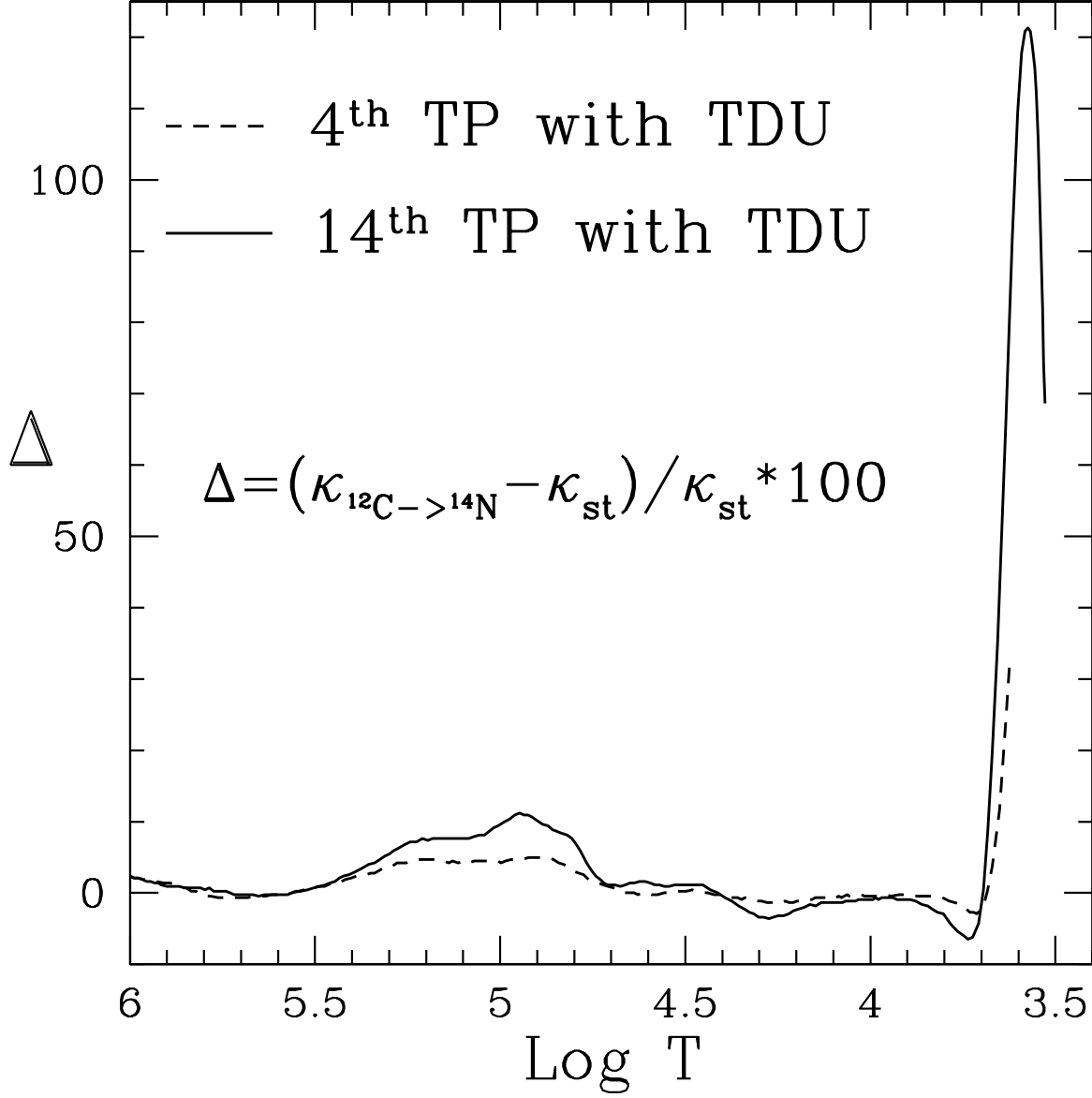


Fig. 7.— Percentage differences of the opacity coefficients calculated in the physical structure of the *CN-int* model after the 4th TP with TDU (dashed line) and after the 14th TP with TDU (solid line); see text for details.

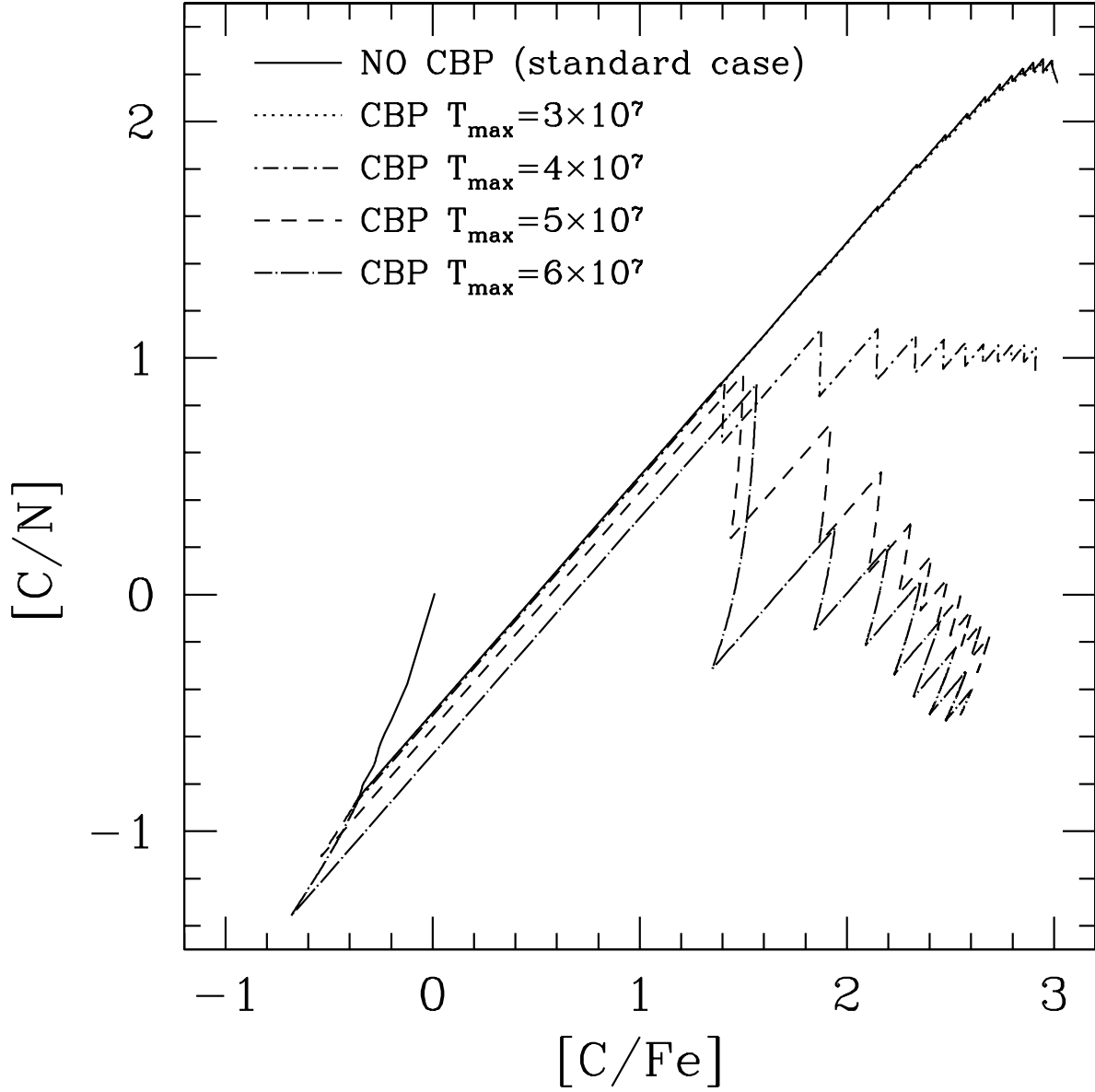


Fig. 8.— $[C/N]$ surface ratios plotted against $[C/Fe]$ for different CBP efficiencies. See text for details.